JOURNAL OF
EMERGING INVESTIGATORS

Article

Hammett linear free-energy relationships in the biocatalytic hydrolysis of para-substituted nitrophenyl benzoate esters

Selin Kocalar[1], Catherine Zhou[2], Jadon Tan[3], Alex Liu[3], Elliott Chen[3], Aylin Salahifar[4], Pranjal Verma[5], Saanvi Pemmaraju[3], Edward Njoo[6]

[1]Leigh High School, San Jose, CA
[2]Lynbrook High School, San Jose, CA
[3]Mission San Jose High School, Fremont, CA
[4]Carlmont High School, Belmont, CA
[5]Dougherty Valley High School, San Ramon, CA
[6]Department of Chemistry, Biochemistry, & Physical Science, Aspiring Scholars Directed Research Program, Fremont, California

SUMMARY

As the drive toward more efficient, sustainable, and affordable methods of chemical synthesis continues, the focus on biocatalysts has grown significantly. Using the Hammett linear free-energy relationship (LFER), we can gain mechanistic insight into chemical transformations such as those catalyzed by enzymes. In this study, we investigated the catalytic mechanisms of trypsin, lipase, and nattokinase by using the Hammett LFER to compare the electronic effects of various para-substitutions on ester hydrolysis. We synthesized a class of nitrophenyl benzoate esters with electron-withdrawing and electron-donating para-substituents and subjected them to enzymatic hydrolysis, from which we obtained kinetic data by spectroscopically tracking the release of 4-nitrophenol, a bright yellow compound that forms upon hydrolysis. We then used the Hammett equation to analyze kinetic trends, and further supported our study with computational modeling, through which a direct correlation between the carbonyl carbon Mulliken charge and the σ_{para} constant was established. These results suggest that the hydrolysis reaction, when catalyzed by either of the three enzymes, exhibited a change in the rate-determining step. We also observed relative differences in enzymatic sensitivity to substrate electronic effects and enzymatic ability to stabilize charged intermediates.

INTRODUCTION

Through the search for efficient and green methods of chemical synthesis, much focus has been brought to nature's arsenal of sustainable, biodegradable, and accessible catalysts: enzymes. Traditionally, organo- and organometallic catalysts have been used to increase the rate of reactions by lowering the required activation energy (1). However, these catalysts come with drawbacks as they lack specificity for substrates, do not always exhibit high catalytic power, and can pose serious environmental or safety hazards (2). Thus, enzymes have been increasingly used as biocatalysts, allowing for the design of biocatalytic cascades, or sequences of enzyme-catalyzed reactions where the product of one enzymatic step becomes the substrate of another, which reduces waste and eliminates the need to isolate intermediates (3).

Biocatalysts have already attracted much attention in synthetic organic chemistry. In 2019, Huffman and colleagues engineered a total synthesis route comprising nine enzyme-mediated transformations to obtain the anti-HIV drug Islatravir, streamlining a synthetic route that otherwise consists of twelve to eighteen steps (4). These catalysts have also shown promising implications in industrial settings, such as in the transesterification of vegetable oil to produce biodiesel (5). To further utilize the benefits of biocatalysts, more research is required to better understand enzymatic mechanisms and how enzymes should be selected depending on their substrates' stereoelectronic properties (6).

Hammett linear free-energy relationships (LFER) have historically been used to elucidate free energy landscapes in reaction mechanisms by harnessing differences in reactivity of substituted aromatic substrates, most commonly para- or meta-substituted benzoic acids and their derivatives (7). The mathematical relationship obtained in *Equation 1* (the Hammett equation) describes the increase or decrease of a reaction rate given a set of aryl substituents as a linear function of the substituent constant, σ, and the reaction constant, ρ (**Table 1**) (8). Relative changes in reactivity are defined by k, the reaction rate of a substituted reactant, and k_0, the reference constant when a hydrogen atom is in place

$$log(\frac{k}{k_0}) = \sigma\rho \qquad (1)$$

para-substituent	σ_{para} constant
NO_2	0.778
Br	0.232
Cl	0.227
F	0.0620
H	0.00
Me ($-CH_3$)	-0.170
OMe ($-OCH_3$)	-0.268

Table 1. The corresponding Hammett σ_{para} constants of various benzene para-substituents. The values range from electron-withdrawing (NO_2, 0.778) to electron-donating functional groups (OMe, -0.268).

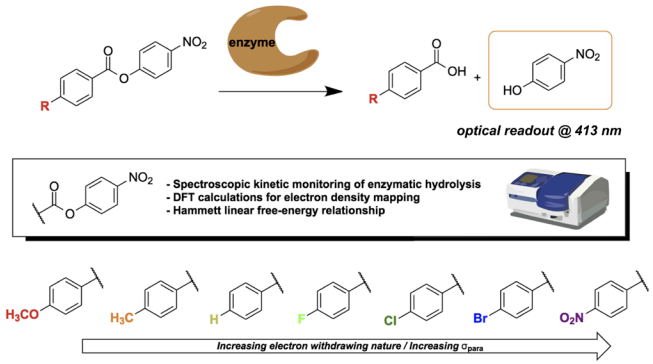

Figure 1. Graphical abstract of using 4-nitrophenyl ester colorimetric probes to identify LFERs in biocatalytic trends. The kinetics of enzymatic hydrolysis of ester bonds is largely governed by stereoelectronic factors, and trends in the relative electronic effects of para-substituted benzoate esters can be modeled using the Hammett LFER. Kinetic data can be spectroscopically obtained by monitoring the release of 4-nitrophenol, a product of hydrolysis with an optical readout.

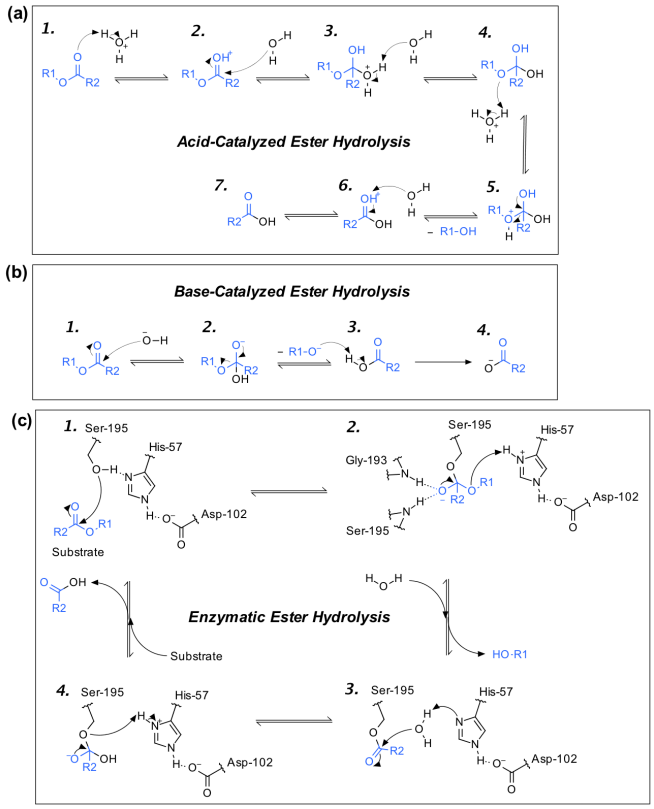

Figure 2. Non-enzymatic and enzymatic hydrolysis of ester bonds. All mechanisms involve a nucleophilic attack resulting in the formation of a tetrahedral intermediate, followed by the collapse of that intermediate to yield the corresponding products. (**a**) Acid-catalyzed hydrolysis of ester bonds. (**b**) Base-catalyzed hydrolysis of ester bonds. (**c**) Enzymatic hydrolysis of ester bonds. The catalytic triad found in serine proteases and esterases consists of three residues: serine-195, histidine-57, and aspartate-102. The histidine engages the serine residue in a hydrogen bonding network, which enhances its nucleophilicity. Upon nucleophilic addition, the serine forms a tetrahedral intermediate with the substrate, and collapse of this intermediate yields an alcohol and a carboxylic acid.

of the substituent.

While this equation has classically been applied to common organic reactions such as acylations and ester hydrolysis, there have also been previous reports of utilizing Hammett relationships to probe the activity of enzymes (9). Here, we used the Hammett LFER to model the relative electronic effects of 4-substituted benzoate esters on enzyme hydrolysis kinetics (**Figure 1**).

We subjected these compounds to enzymatic hydrolysis by trypsin, a serine protease that hydrolyzes proteins in the digestive system; pre-gastric lipase, an esterase that hydrolyzes lipids; and nattokinase, a serine protease that catabolizes a variety of substrates (15-17). We also monitored non-enzymatic hydrolysis in various pH conditions to compare the kinetic trends of biocatalysis to that of acidic and basic catalysis. The hydrolytic mechanism of the three enzymes studied utilizes a catalytic triad in the enzyme active site, in which a residue acting as a nucleophile, specifically serine, performs covalent catalysis of the substrate to cleave its ester bond (10). The nucleophilic residue is oriented and stabilized by the other triad members, which in turn increases its reactivity (**Figure 2**).

We hypothesized that initial nucleophilic addition of the active site nucleophile would be the rate-determining step in this mechanism, and therefore more electron-withdrawing para-substituents, which increase the electrophilic nature of the carbonyl, would accelerate the hydrolysis reaction. We further hypothesized that there would be a direct correlation between reaction rate and charge density at the carbonyl carbon, where more electron-withdrawing para-substituents would decrease charge density at the carbonyl carbon and increase the rate of initial nucleophilic attack. After collecting spectroscopic data, Hammett plots were constructed, comparing the effects of electron-withdrawing and electron-donating functional groups on the rate of hydrolysis. Contrary to initial expectations, the kinetic data obtained did not fit linearly with the electron-withdrawing nature of the para-substituent, and a change in the rate-determining step from the initial nucleophilic attack to the collapse of the tetrahedral intermediate was observed.

RESULTS

To monitor the kinetics of enzymatic hydrolysis, we used nitrophenyl esters as colorimetric substrates (11). Once cleaved, these substrates release 4-nitrophenol, a bright yellow compound that can be tracked on a spectrophotometer by an optical readout at 413 nm. 4-nitrophenyl acetate is one such commercially-available substrate that has been widely used for monitoring enzymatic activity (12-14). We chemically synthesized seven 4-nitrophenyl benzoate esters with various substituents at the para-position: 4-nitrophenyl benzoate and the corresponding 4-substituted 4-nitrophenyl benzoate esters with nitro, bromo, chloro, fluoro, methyl, and methoxy functional groups at the benzoate para-position. These were strategically chosen as each of these functional groups exhibits an electron-donating or electron-withdrawing effect of a different degree, ranging from para-nitro (σ_{para} = 0.778),

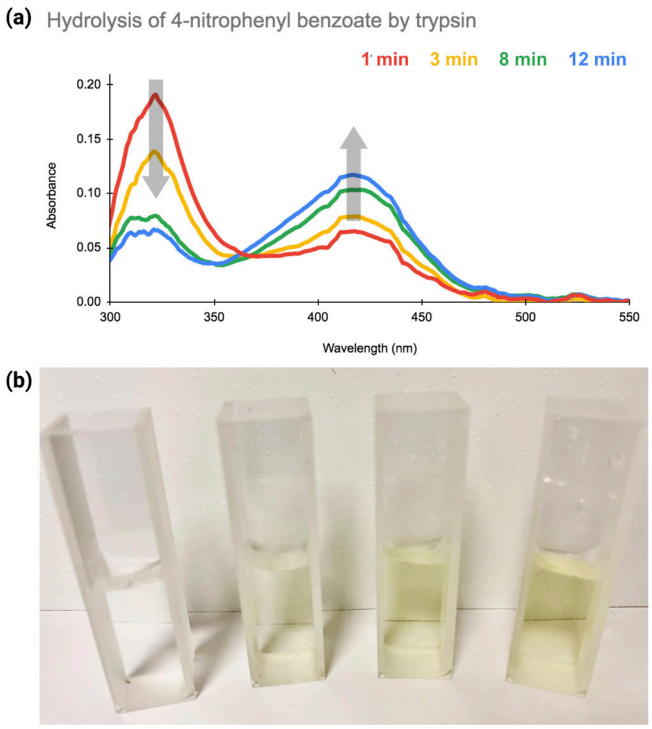

Figure 3. Reaction kinetic data were collected by monitoring the change in absorbance due to the production of 4-nitrophenol. (**a**) Absorbance spectrum of 4-nitrophenyl benzoate cleaved by trypsin at time intervals of 1 min, 3 min, 8 min, and 12 min, showing increases in absorbance at 413 nm (belonging to 4-nitrophenol) and decreases in absorbance at ~350 nm (belonging to 4-nitrophenyl benzoate). (**b**) Cuvettes containing hydrolysis products of 4-nitrophenyl benzoate by trypsin, showing increasing yellow color, due to an increasing concentration of 4-nitrophenol. Left to right: 1 min, 3 min, 8 min, 12 min after reaction with trypsin.

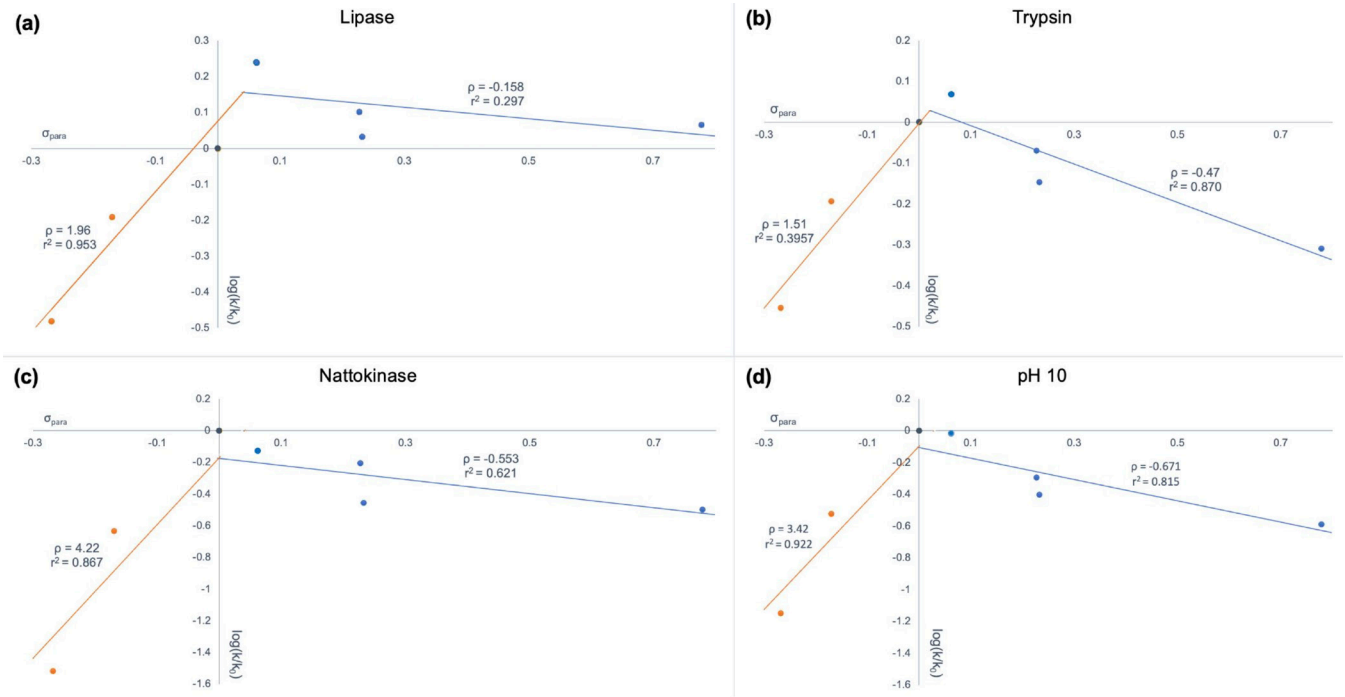

Figure 4. Hammett plots of various para-substituted 4-nitrophenyl benzoate esters under different hydrolysis conditions. Points representing electron-donating substituents are shown in orange, reference points representing no substituent (hydrogen atom) in gray, and points representing electron-withdrawing substituents in blue. All data were highly reproducible, as the standard deviations for all log(k/k_0) values were between 0.0000948 and 0.00226. (**a**) Hammett plot for trypsin. (**b**) Hammett plot for lipase. (**c**) Hammett plot for nattokinase. (**d**) Hammett plot for pH 10 conditions.

which is the most electron-withdrawing, to para-methoxy, which is the most electron-donating (σ_{para} = -0.268).

Substrates were synthesized and subjected to hydrolysis by lipase, trypsin, and nattokinase, as well as non-enzymatic hydrolysis in pH 1, 4, 10, and 14 conditions. As 4-nitrophenol was produced through the hydrolysis reaction, the absorbance at 413 nm and the intensity of the yellow color increased (**Figure 3**).

We used the spectroscopic data to derive reaction kinetics, and then modeled reaction kinetics with the

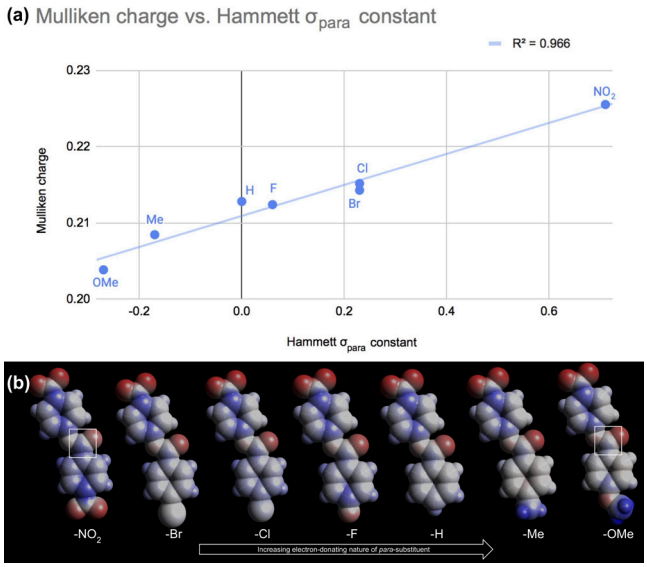

Figure 5. Carbonyl carbon Mulliken charges were calculated to identify relationships between charge density at the reaction center and rate of hydrolysis. (**a**) The linear relationship between the Hammett σpara constant and Mulliken charge at the carbonyl carbon of each substrate. The Mulliken charges for NO_2, Br, Cl, F, H, Me, and OMe para-substituents were 0.2255, 0.2151, 0.2143, 0.2124, 0.2128, 0.2084, and 0.2038, respectively. (**b**) Van der Waals surfaces of each substrate, with electron-poor surfaces shown in blue and electron-rich surfaces shown in red. As the para-substituent became increasingly electron-donating, the carbonyl carbon became more electron-rich.

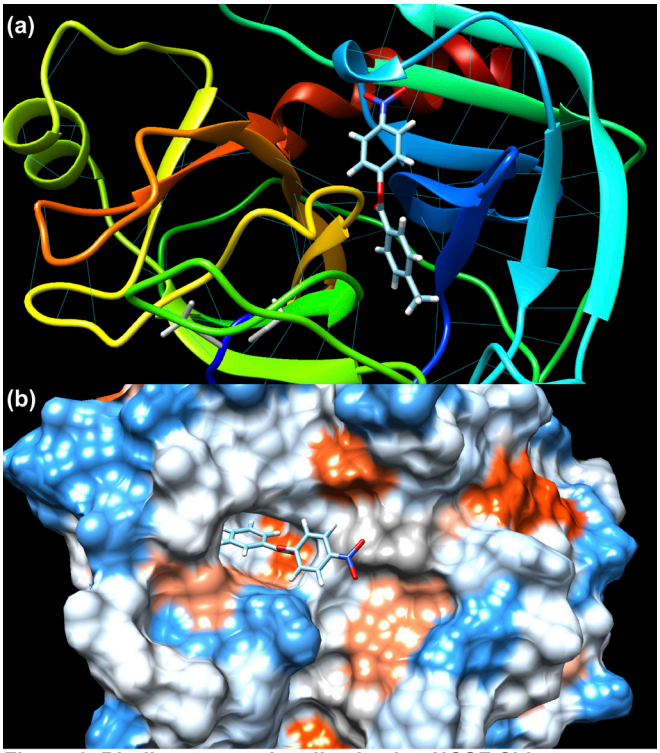

Figure 6. Binding poses visualized using UCSF Chimera indicate that the para-substituent does not directly interact with the active site but instead affects hydrolysis through inductive effects. This is consistent with the observed trend that experimentally-obtained binding energies do not inform hydrolysis kinetics. a) General binding pose in the enzyme active site, showing 4-nitrophenyl 4-methylbenzoate bound to trypsin. b) Hydrophobic/hydrophilic interactions in the enzyme active site, showing 4-nitrophenyl benzoate bound to trypsin.

Lowest ΔG (best binding affinity, kcal/mol)			
Substrate	**Trypsin**	**Lipase**	**Nattokinase**
4-nitrophenyl 4-nitrobenzoate	-6.69	-7.12	-7.15
4-nitrophenyl 4-bromobenzoate	-7.16	-6.88	-7.21
4-nitrophenyl 4-chlorobenzoate	-6.98	-6.84	-7.17
4-nitrophenyl 4-fluorobenzoate	-7.10	-6.93	-7.00
4-nitrophenyl benzoate	-7.30	-6.89	-6.84
4-nitrophenyl 4-methylbenzoate	-7.19	-6.63	-7.09
4-nitrophenyl 4-methoxybenzoate	-7.04	-6.87	-7.02

Table 2. Best binding affinities between each substrate and enzyme studied. The values show no significant difference in binding affinity among substrates with varying electronic properties.

Hammett equation (**Figure 4**). Hammett plots were only able to be generated in basic conditions as all substrates were highly stable under acidic conditions. Contrary to the initial hypothesis, the Hammett plots for all three enzymes exhibited a downward concavity, indicating that the charge density at the carbonyl carbon did not directly correlate to the rate of enzymatic hydrolysis (18,19). The inflection points in the Hammett plots for trypsin, lipase, nattokinase, and pH 10 conditions were (0.021, 0.0288), (0.0406, 0.1556), (0.0113, -0.1253), and (-0.0033, -0.1108), respectively. All inflection points for enzymatic hydrolysis plots were located between the σ_{para} constant of hydrogen and fluorine para-substituents, whereas the inflection point under pH 10 conditions was located between the σ_{para} constant of methyl and hydrogen para-substituents.

Furthermore, Mulliken charges at the carbonyl carbon, which represent the local charge density, were determined using density-functional theory (DFT), a quantum mechanical method that uses an electron density functional to predict the energy of a system (**Figure 5**). Since we hypothesized that these charges would play a key role in the rate of hydrolysis, we further rationalized that there would be a correlation between the Hammett σ_{para} constant and the Mulliken charge. Electronic density was also visualized on Avogadro, a platform for viewing chemical structures, confirming that electron-withdrawing groups decreased the charge density of the carbonyl carbon, and vice versa (20).

Finally, molecular docking simulations were conducted

to assess substrate-enzyme binding affinity. The binding affinities for all substrate-enzyme pairs proved to be highly similar, suggesting that electronic properties, in addition to binding energies, play a role in the rate of hydrolysis (**Table 2**, **Figure 6**).

DISCUSSION

Through our studies, we synthesized a class of 4-nitrophenyl ester substrates, then spectroscopically monitored their hydrolysis by three enzymes and in varying pH conditions. We used this spectroscopic data to derive reaction kinetics, then constructed Hammett plots to model the kinetic trends. We paralleled these efforts with computational studies, and found no correlation between hydrolytic rates and binding affinity, but rather a correlation with hydrolytic rates and carbonyl carbon charge density.

The inflection points observed in all Hammett plots are indicative of a change in the rate-determining step. When the para-substituent is electron-donating, the rate-determining step is the nucleophilic attack; since the transition state involves a buildup of negative charge, less electron-donating substituents increase the rate of attack onto the carbonyl carbon. However, when the para-substituent becomes electron-withdrawing, the rate-determining step is no longer the nucleophilic attack but rather the collapse of the tetrahedral intermediate; more electron-withdrawing functionalities stabilize the tetrahedral intermediate by removing electron density from the reaction center, thus reducing the overall rate of hydrolysis.

The shifts in the Hammett plot inflection points also offer interesting mechanistic insight, and may be caused by the enzymes' differing abilities to stabilize the tetrahedral intermediate, thereby altering the point of change in the rate-determining step. The inflection point of lipase occurs later than that of trypsin, whose inflection point is later than that of nattokinase. This may indicate that nattokinase is the best at stabilizing the tetrahedral intermediate, which reduces the rate at which it is able to hydrolyze substrates with electron-withdrawing functionalities. Finally, lipase was able to cleave all substrates with electron-withdrawing functionalities at a faster rate than 4-nitrophenyl benzoate (ρ = -0.158), which may be because lipase is less sensitive to inductive effects, whereas trypsin gave the steepest decrease in hydrolysis with increasingly electron-withdrawing functionalities (ρ = -0.470), suggesting that the enzyme has the greatest sensitivity to inductive effects in the stabilization of the tetrahedral intermediate.

Consistent with expectation, Mulliken charges at the carbonyl carbon reaction center obtained by DFT calculations showed a linear correlation with previously-reported Hammett σ_{para} values, where more electron-withdrawing functionalities at the para position were predicted to have more electron-poor carbonyls, and vice versa. Docking simulation results did not yield any significant differences in predicted binding affinities for each of the enzymes' active sites. This suggests

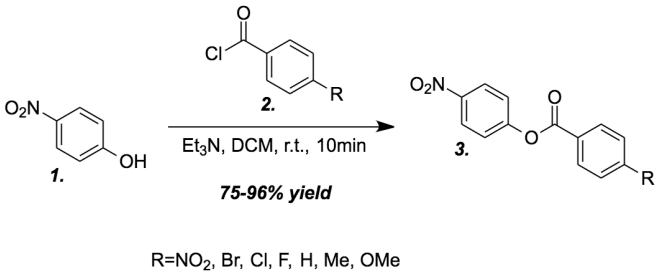

Figure 7. General procedure for the acylation of 4-nitrophenol. This was done via a 4-substituted benzoyl chloride (1). Upon purification (2), 4-nitrophenyl benzoyl esters (3) were afforded in 75-96% yield.

that the identity of the para-substituent on each compound has a minimal effect on substrate binding affinities, and that differences in enzymatic hydrolysis are a result of differences in substrate electronics conferred by the para-substituent rather than the intrinsic stability of the enzyme-substrate complex.

In this study, we gained mechanistic insight into the catalytic triads of trypsin, lipase, and nattokinase, including insight into their ability to stabilize charged intermediates and their sensitivity to electronic effects. We also demonstrated that substituent groups that were the least electron-withdrawing or electron-donating resulted in the quickest rate of hydrolysis because they had the least rate-limiting effect. Hence, the results from this study inform future efforts of the feasibility of using the Hammett LFER to model biocatalytic transformations to monitor kinetic trends and to probe relative differences in enzymatic active sites. In the future, we plan on using related LFERs to model steric effects on biocatalytic efficiency.

METHODS

Chemical synthesis

We synthesized each of the 4-nitrophenyl benzoate esters via acylation of 4-nitrophenol [Reagent Inc. (>98%)] by a 4-substituted benzoyl chloride (**Figure 7**). 4-nitrophenol (0.25g, 1 eq., 3.6 mmol) was dissolved in methylene chloride and added to a round-bottom flask equipped with a Teflon stir bar, along with 1 eq. triethylamine. The flask was then septum-sealed and stirred until 4-nitrophenol had dissolved completely. One eq. of the respective 4-substituted benzoyl chloride was then added to the reaction mixture and the reaction was monitored to completion via thin-layer chromatography (TLC). The crude reaction mixture was concentrated in vacuo and purified using silica gel flash chromatography with a gradient of 0-30% ethyl acetate in hexanes, yielding off-white crystals of 4-nitrophenyl 4-substituted benzoates in 75% to 96% yield. 4-nitrophenyl 4-nitrobenzoate (96% yield), 4-nitrophenyl 4-bromobenzoate (95% yield), 4-nitrophenyl 4-chlorobenzoate (94% yield), 4-nitrophenyl 4-fluorobenzoate (75% yield), 4-nitrophenyl benzoate (81% yield), 4-nitrophenyl 4-methylbenzoate (96% yield), and 4-nitrophenyl 4-methoxybenzoate (95% yield) were synthesized in this manner. All solvents were purchased

from Stellar Chemical, JT Baker, or Fisher, and used without further purification.

All compounds were characterized by ^{1}H, $^{13}C\{^{1}H\}$, and ^{19}F NMR [Nanalysis NMReady 60 MHz nuclear magnetic resonance spectrometer in deuterated chloroform (Cambridge Isotope Laboratories, >99.8% D, 0.1% tetramethylsilane (TMS) as an internal standard)], Fourier-transform infrared (FT-IR) spectroscopy (Thermo Scientific iS5 Nicolet FT-IR spectrometer, iD5 ATR assembly), and ultraviolet-visible spectroscopy (BioRad SmartSpec 3000 UV-vis spectrophotometer, quartz cuvette). Full characterization and spectroscopic data are available in the Supplementary Information document.

UV-visible spectroscopy

A Beer's Law plot of 4-nitrophenol was produced by collecting spectroscopic data at various micromolar concentrations using a Spectronic Genesys 5 UV-Vis spectrophotometer. 4-nitrophenol was prepared in 10% dimethyl sulfoxide (DMSO, DMSO Store, 99.995%) and 90% 10 mM Tris buffer at concentrations of 1.25 µM, 2.5 µM, 5 µM, and 10 µM. The peak absorbance of 4-nitrophenol was determined to be at 413 nm, which did not overlap with the absorption spectra of any of the substrates.

Enzyme and substrate solutions were prepared separately, then added into a glass cuvette together to monitor the rate of enzymatic hydrolysis. One millimolar substrate solutions of each of the seven compounds were prepared in DMSO, and enzyme solutions at pH 8 were prepared with 1 mM Tris base in deionized water and 0.5 mg enzyme per 1 mL of solution. Trypsin was purchased from Bio-Rad, lipase was purchased from Carolina Biological, and nattokinase was purchased from Belle Chemical. Once 1800 µL enzyme solution was added to 200 µL substrate solution in a glass cuvette, the absorbance at 413 nm was measured every minute for 12 minutes. When testing the substrates' hydrolysis in various pH conditions, the same procedure was repeated but separate solutions at pH 1, 4, 10, and 14 were used in place of enzyme solutions. These varying pH solutions were prepared with 1 mM Tris base (HiMedia) in deionized water and HCl for acidic solutions, and 5 mM and 7 mM Tris base in deionized water for basic solutions of pH 10 and 14, respectively. Blank spectra were also taken for each of the substrates with 1 mM Tris buffer instead of enzyme or pH solution to account for hydrolysis of the substrate by deionized water. Blank readings were subtracted from readings collected from samples undergoing enzyme- or pH-mediated hydrolysis and all experiments were repeated in triplicate.

The rate of hydrolysis of each substrate by each enzyme and pH condition was determined by calculating the average rate of increase of the concentration of 4-nitrophenol in nm/min over the first 12 minutes of hydrolysis. Average rate data were then inputted into the Hammett equation and graphed alongside the Hammett σ_{para} constant (8).

Computational modeling

Each substrate was constructed virtually in Avogadro and optimized using DFT by ORCA (21). Mulliken charges at the carbonyl carbon were identified using these DFT calculations. Subsequently, molecular docking was performed in Swissdock to identify the binding affinities between the substrates and three enzymes tested, which were trypsin (PDB: 1S0Q), with the grid box center having coordinates (7.906, 3.389, 35.952) and the gridbox dimensions being (25, 25, 25); lipase (PDB: 1N8S) with the grid box center having coordinates (12.188, 20.152, 48.922) and the gridbox dimensions being (72, 72, 72); and nattokinase (PDB: 4DWW) with the grid box center having coordinates (19.535, 9.188, 7.963) and the gridbox dimensions being (9, 7, 10) (22–24). UCSF Chimera was used to analyze post-docking results.

Computational simulations and DFT calculations were performed on a Dell Poweredge 710 server with a 24 core Intel Xeon X5660 processor @ 2.80GHz and 32GB RAM. In all DFT calculations, CPCM implicit solvation with the dielectric constant of water was used as the solvation model, B3LYP was used as the functional, and def2-SVP was used as the basis set (25).

ACKNOWLEDGEMENTS

We would like to thank the Aspiring Scholars Directed Research program for providing us with lab space as well as the opportunity to conduct high-quality research. We would also like to thank the lab technicians for ensuring our safety and helping us resolve technical issues while in the laboratory. Last but not least, we gratefully acknowledge the Olive Children Foundation and its community of corporate sponsors and supporters for funding our research.

Received: February 11, 2021
Accepted: June 17th, 2021
Published: July 18, 2021

REFERENCES

1. Truppo, Matthew D., *et al*. "Biocatalysis in the Pharmaceutical Industry: The Need for Speed." *ACS Med. Chem. Letters*, vol. 8, no. 5, 2017, pp. 476-480., doi: 10.1021/acsmedchemlett.7b00114.
2. Sheldon, Roger A., *et al*. "Engineering a more sustainable world through catalysis and green chemistry." J*ournal of The Royal Society Interface*, vol. 13, no. 116, 2016, pp. 20160087., doi: 10.1098/rsif.2016.0087.
3. France, Scott P., *et al*. "Constructing Biocatalytic Cascades: In Vitro and in Vivo Approaches to de Novo Multi-Enzyme Pathways." *ACS Catalysis*, vol. 7, no. 1, 2017, pp. 710-724., doi: 10.1021/acscatal.6b02979.
4. Huffman, Mark A., *et al*. "Design of an in vitro biocatalytic cascade for the manufacture of islatravir." *Science*, vol. 366, no. 6470, 2019, pp. 1255-1259., doi: 10.1126/science.aay8484.
5. Thangaraj, Baskar, *et al*. "Catalysis in biodiesel

production—a review." *Clean Energy*, vol. 3, no. 1, 2018, pp. 2-23., doi: 10.1093/ce/zky020.
6. Domínguez de María, Pablo, *et al*. "On the (Un)greenness of Biocatalysis: Some Challenging Figures and Some Promising Options." *Frontiers in Microbiology*, vol. 6 no. 1257, 2015, pp. 1257., doi: 10.3389/fmicb.2015.01257.
7. Mustafa, Damra, *et al*. "Kinetic Study of the Reaction of Benzofuroxans with 2-Acetylthiophene: Effect of the Substituents on the Reaction Rate Using Hammett Equation." *Orbital: The Electronic Journal of Chem.*, vol. 12, no. 1, 2020, pp. 24-29., doi: 10.17807/orbital.v12i1.1436.
8. Johnson, Colin D., *et al*. "The Hammett equation." CUP Archive, 1973.
9. Ferguson, Kyle L. *et al*. "Mechanism of the novel prenylated flavin-containing enzyme ferulic acid decarboxylase probed by isotope effects and linear free-energy relationships." *Biochemistry*, vol. 55, no. 20, 2016, pp. 2857-2863, doi: 10.1021/acs.biochem.6b00170.
10. Buller, Andrew R., *et al*. "Intrinsic evolutionary constraints on protease structure, enzyme acylation, and the identity of the catalytic triad." *Proceedings of the National Academy of Sciences of the United States of America*, vol. 110, no. 8, 2013, pp. 653-661., doi: 10.1073/pnas.1221050110.
11. Qian, Le, *et al*. "Fingerprint lipolytic enzymes with chromogenic p-nitrophenyl esters of structurally diverse carboxylic acids." *Journal of Molecular Catalysis B: Enzymatic*, vol. 73, no. 1, 2011, pp. 22-26., doi: 10.1016/j.molcatb.2011.07.010.
12. Der, Bryan S., *et al*. "Catalysis by a de novo zinc-mediated protein interface: implications for natural enzyme evolution and rational enzyme engineering." *Biochemistry*, vol. 51, no. 18, 2012, pp. 3933-3940., doi: 10.1021/bi201881p.
13. Demirdağ, Ramazan, *et al*. "Purification and characterization of carbonic anhydrase from sheep kidney and effects of sulfonamides on enzyme activity." *Bioorganic & Medicinal Chemistry*, vol. 21, no. 6, 2013, pp. 1522-1525., doi: 10.1016/j.bmc.2012.08.018.
14. Ascenzi, Paolo, *et al*. "Pseudo-enzymatic hydrolysis of 4-nitrophenyl acetate by human serum albumin: pH-dependence of rates of individual steps." *Biochemical and Biophysical Research Communications*, vol. 424, no. 3, 2021, pp. 451-455., doi: 10.1016/j.bbrc.2012.06.131.
15. Juyeon, Ko, *et al*. "Low serum amylase, lipase, and trypsin as biomarkers of metabolic disorders: A systematic review and meta-analysis." *Diabetes Research and Clinical Practice*, vol. 159, 2020, pp. 107974., doi: 10.1016/j.diabres.2019.107974.
16. Kumar, Ashok, *et al*. "Lipase catalysis in organic solvents: advantages and applications." *Biological Procedures Online*, vol. 18, no. 2, 2016, pp. 2., doi: 10.1186/s12575-016-0033-2.
17. Cai, Dongbo, *et al*. "Microbial production of nattokinase: current progress, challenge and prospect." *World Journal of Microbiology and Biotechnology*, vol. 33, no. 5, 2017, pp. 84., doi: 10.1007/s11274-017-2253-2.
18. Schreck, James O. "Nonlinear Hammett relationships." *Journal of Chemical Education*, vol. 48, no. 2, 1971, pp. 103., doi: 10.1021/ed048p103.
19. Um, Ik-Hawn, *et al*. "Nonlinear Hammett plots in pyridinolysis of 2, 4-dinitrophenyl X-substituted benzoates: change in RDS versus resonance contribution." *Organic and Biomolecular Chemistry*, vol. 8, no. 16, 2010, pp. 3801-3806., doi: 10.1039/C0OB00031K.
20. Hanwell, Marcus D., *et al*. "Avogadro: an advanced semantic chemical editor, visualization, and analysis platform." *Journal of Cheminformatics*, vol. 4, no. 1, 2012, pp. 1-17., doi: 10.1002/wcms.81.
21. Neese, Frank, *et al*. "The ORCA program system." *Wiley Interdisciplinary Reviews: Computational Molecular Science*, vol. 2, no. 1, 2011, pp. 73-78., doi: 10.1186/1758-2946-4-17.
22. Ruhlmann, Alfred, *et al*. "Structure of the complex formed by bovine trypsin and bovine pancreatic trypsin inhibitor: crystal structure determination and stereochemistry of the contact region." *Journal of Molecular Biology*, vol. 77, no. 3, 1973, pp. 417-436., doi: 10.1016/0022-2836(73)90448-8.
23. Uppenberg, Jonas, *et al*. "The sequence, crystal structure determination and refinement of two crystal forms of lipase B from Candida antarctica." *Structure*, vol. 2, no. 4, 1994, pp. 293-308., doi: 10.1016/S0969-2126(00)00031-9.
24. Yanagisawa, Yasuhide, *et al.* "Purification, crystallization and preliminary X-ray diffraction experiment of nattokinase from Bacillus subtilis natto." *Acta Crystallographica Section F: Structural Bio. and Crystallization Communications*, vol. 66, no. 12, 2010, pp. 1670-1673., doi: 10.1107/S1744309110043137.
25. Takano, Yu, *et al.* "Benchmarking the conductor-like polarizable continuum model (CPCM) for aqueous solvation free energies of neutral and ionic organic molecules." *Journal of Chemical Theory and Computation*, vol. 1, no. 1, 2005, pp. 70-77., doi: 10.1021/ct049977a.